Arch. Metall. Mater. **63** (2018), 4, 1587-1594

DOI: 10.24425/amm.2018.125081

M. AKKAŞ*#, T. ÇETIN**, M. BOZ**

THE EFFECT OF GAS PRESSURE ON POWDER SIZE AND MORPHOLOGY IN THE PRODUCTION OF AZ91 POWDER BY GAS ATOMIZATION METHOD

In this study, the effect of gas pressure on the shape and size of the AZ91 alloy powder produced by using the gas atomization method was investigated experimentally. Experiments were carried out at 820°C constant temperature in 2-mm nozzle diameter and by applying 4 different gas pressures (0.5, 1.5, 2.5 and 3.5 MPa). Argon gas was used to atomize the melt. Scanning electron microscope (SEM) to determine the shape of produced AZ91 powders, XRD, XRF and SEM-EDX analysis to determine the phases forming in the internal structures of the produced powders and the percentages of these phases and a laser measuring device for powder size analysis were used. Hardness tests were carried out to determine the mechanical properties of the produced powders. The general appearances of AZ91 alloy powders produced had general appearances of ligament, acicular, droplet, flake and spherical shape, but depending on the increase in gas pressure, the shape of the powders is seen to change mostly towards flake and spherical. It is determined that the finest powder was obtained at 820°C with 2 mm nozzle diameter at 3.5 MPa gas pressure and the powders had complex shapes in general.

Keywords: Gas atomization, AZ91 alloy powder, gas pressure, powder morphology

1. Introduction

Magnesium represents the lightest engineering metal with a density of 1.74 g/cm^3, which is 35% lower than aluminum and 75% lower than iron from the main building metals in use [1,2]. Compared to these metals, magnesium has a similar specific hardness and advantages such as higher specific strength and a high absorption capacity [1,3]. However, magnesium has some disadvantages that limit its use as engineering material. Especially at high temperatures, its creep resistance and mechanical strength are relatively low [1]. Secondly, due to its crystal structure, the hexagonal close packing (HSP) provides very low ductility and formability [4]. In addition, magnesium has the high oxidation sensitivity and the tendency to have a strong chemical reaction and it can sometimes lead to spontaneous combustion [5,6]. Therefore, they are usually alloyed with elements such as aluminum, zinc, zirconium and rare earth elements in order to increase the strength, corrosion, and fire resistance of magnesium [7,8]. Magnesium alloys can be divided into two broad categories as containing aluminum and aluminum free one depending on whether it was alloyed with aluminum [9-11]. AZ series alloys are the most common magnesium alloys due to their low cost, improved corrosion resistance and high mechanical strength achieved by the addition of aluminum, zinc and manganese [12-14]. In this alloy family, AZ91 alloy seems to have optimum structural strength because it tends to precipitate from the magnesium matrix to form dual precipitates with aluminum and manganese [15,16]. In addition, since it will increase the strength in these materials having fine microstructure, the production of the materials with low formability like magnesium and their alloys with powder metallurgy has become a need.

Powder metallurgy has been developed as an alternative to the manufacturing methods such as casting, hot and cold pressing, machining. Since coarse-structured microstructures are produced by casting method, powder metallurgy is considered an effective way to encourage a finer microstructure [17,18]. By obtaining composites by using powder metallurgy method, properties such as increasing surface wear resistance, surface friction and surface tensions can be brought to the materials at high temperature [19-22]. Powder production technique with powder metallurgy method is done by 4 different methods. These are mechanical methods, chemical methods, electrolysis method, and atomization method. Among these production methods, gas atomization method is most widely used one to obtain fine and spherical powders. The most important reason to want spherical powder is that powder-powder contact in pressing and sintering stages is required to be homogeneous and multi-directional [23].

Atomization is defined as the degradation and solidification of molten metal into very small droplets with water, air and gas

* KASTAMONU UNIVERSITY, CIDE RIFAT ILGAZ VOCATIONAL HIGH SCHOOL, KASTAMONU, TURKEY
** KARABÜK UNIVERSITY, FACULTY OF TECHNOLOGY, DEPARTMENT OF MANUFACTURING ENGINEERING, KARABÜK, TURKEY
# Corresponding author: mehmetakkas@kastamonu.edu.tr

pressures or mechanically. Therefore, atomization process is divided into 4 different parts including, water atomization, gas atomization, centrifugal atomization, and vacuum atomization. However, the production of more than 60% of the metal and nonmetallic powders with gas atomization makes this method superior. Gases such as air, nitrogen, argon and helium can be used as pressurized fluid to decompose the liquid metal bundle in gas atomization [24]. In fact, it is possible to produce all kinds of metal and alloy powders that can be melted by using gas atomization method.

In powder production by gas atomization method; parameters such as gas type, gas pressure, nozzle diameter and melting temperature are used. As the gas pressure increased, the temperature and viscosity of the molten material decrease, which allows the production of smaller size powders [25-27].

2. Materials and methods

For this study, a new gas atomization system, shown in Fig. 1, was designed and manufactured. For the powder production, AZ91 alloy was obtained in the mass from Varzene Metal A.S. and Table 1 shows the chemical composition of the obtained material. Determination of chemical composition was made by XRF (X-Ray Fluorescence Spectroscopy) analysis. Powder production at different gas pressures was performed by using argon gas in AZ91 alloy powder production. As a result of powder production studies, the effect of gas pressure on the particle size and distribution and the shape of the produced powders were investigated.

TABLE 1

Chemical composition of AZ91 ingot

Element	Content (%)
Mg	90,3
Al	8,74
Zn	0,67
Mn	0,18
Fe	0,01
Ni	0,0062

2.1. Gas atomization unit

Gas Atomization Unit consists of 7 basic parts: Melting furnace, Atomization tower, Nozzle and nozzle holder, Powder collecting unit, Gas pressure ramp, Cyclones, and Control panel.

The atomization tower was made of stainless steel in such a way that it would not hit the wall of the tower during the atomization of the powders. Produced powders were gathered in the powder collection unit located at the bottom of the atomization tower. For the discharge of the gas used from the atomization tower and the retention of fine powders, two cyclones connected in serial to each other were designed. During the atomization process, three argon tubes were connected to the gas ramp to

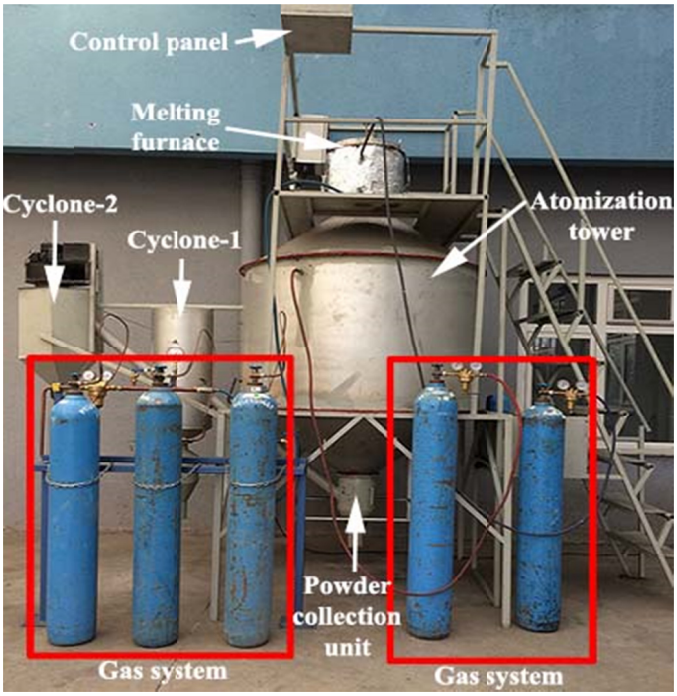

Fig. 1. Gas atomization unit

prevent the change in the gas pressure and fluctuation when the gas pressure decreased in the tube. Method of measurement and adjustment of the gas pressure was made by manometer. Melting process was carried out in a stainless steel crucible placed in the furnace. The temperature of the molten material was measured by means of two thermocouples (Type K), one of which was immersed in a stainless steel crucible and the other one was located outside the crucible.

The melting furnace was designed in such a way to operate continuously at approximately 1200°C. During the melting process, gas inlet and outlet units were installed on the sides of the melting furnace in order to form a shielding gas medium and to prevent the formation of oxide during and after the time of atomization. In order to control the flow of molten metal in the crucible, a graphite plug was used with the worm gear system. A closely matched and circular slotted supersonic nozzle holder was used to atomize the liquid metal. The distance between outlet jet and furnace was 3 mm. The angle of outflow of the gas was 42 degrees. The liquid metal performs a free fall through the exit of the nozzle. Type of the jet was a ring and circular holey supersonic nozzle. The nozzle was placed on the nozzle holder in the furnace.

2.2. Atomization studies

Within the scope of the experimental studies carried out in the atomization unit, AZ91 powder was produced using argon gas. AZ91 alloy found in ingot was heated to 820°C in a stainless steel crucible in a melting furnace and held at this temperature for 1 hour. The melt was then atomized at 2 mm nozzle diameter and at gas pressures of 0.5, 1.5, 2.5 and 3.5 MPa.

2.3. Analysis of atomized powder

Powder size analyses were performed by using the Mastersizer 3000 model device at the Bartın University Central Research Laboratory. The working principle of the device is that red and blue laser lights are sent on the sample. Particle size analysis was made according to ISO 13320:2009 standard with Mie theory.

The SEM images and EDX analyses of the produced AZ91 alloy powders were taken from the "Carl Zeiss Ultra Plus Gemini Fesem" brand device from Karabuk University Institute of Iron and Steel Research Laboratories. The powders were poured on "carbon tape" and coated with gold for the images taken from SEM.

Crystalline phases present in gas atomized powders were determined by X-ray diffractometry (XRD, RIGAKU-Ultima IV). In the chemical analysis of produced AZ91 alloy powder, X-ray fluorescence spectrometry (RIGAKU ZSX Primus II) was used.

In order to measure the hardness of the produced powders, the powders were firstly pelletized with ATLAS GS15011 device. The hardness of the pelletized AZ91 powders was measured using Vickers $HV_{0,5}$ method with the Q250 M Universal Hardness Measurement device.

3. Experimental results and discussion

3.1. Powder size and distribution

The particle size values of the produced AZ91 alloy powders (as taken from the atomization unit) are shown as 10% ($D_{v,10}$), 50% ($D_{v,50}$), 90% ($D_{v,90}$) of the volume distribution and span values in Table 2. In addition, the specific surface area is seen in Table 2 in order to determine the powder type depending on the variables and to support the SEM images in Fig. 2.

Gas pressure is known to have an important effect on the size and shape of the powder in the powder production with gas atomization method. As is seen in Table 2, the highest gas pressure value in this study was taken as 3.5 MPa. Powder production cannot be performed because the gas charged on the nozzle over this pressure formed reverse pressure (positive pressure) in the flow direction of the liquid metal from inside the nozzle. Aydın and Unal [25] emphasized in their study on the effect of production variables on metal powder production that the positive pressure values forming at the end of the flow pipe during the atomization process would slow down the liquid metal flow, Bostan and Gökmeşe [26] stated in a similar study that liquid flow stopped or realized in the reverse direction in some cases. However, it was observed that this condition did not

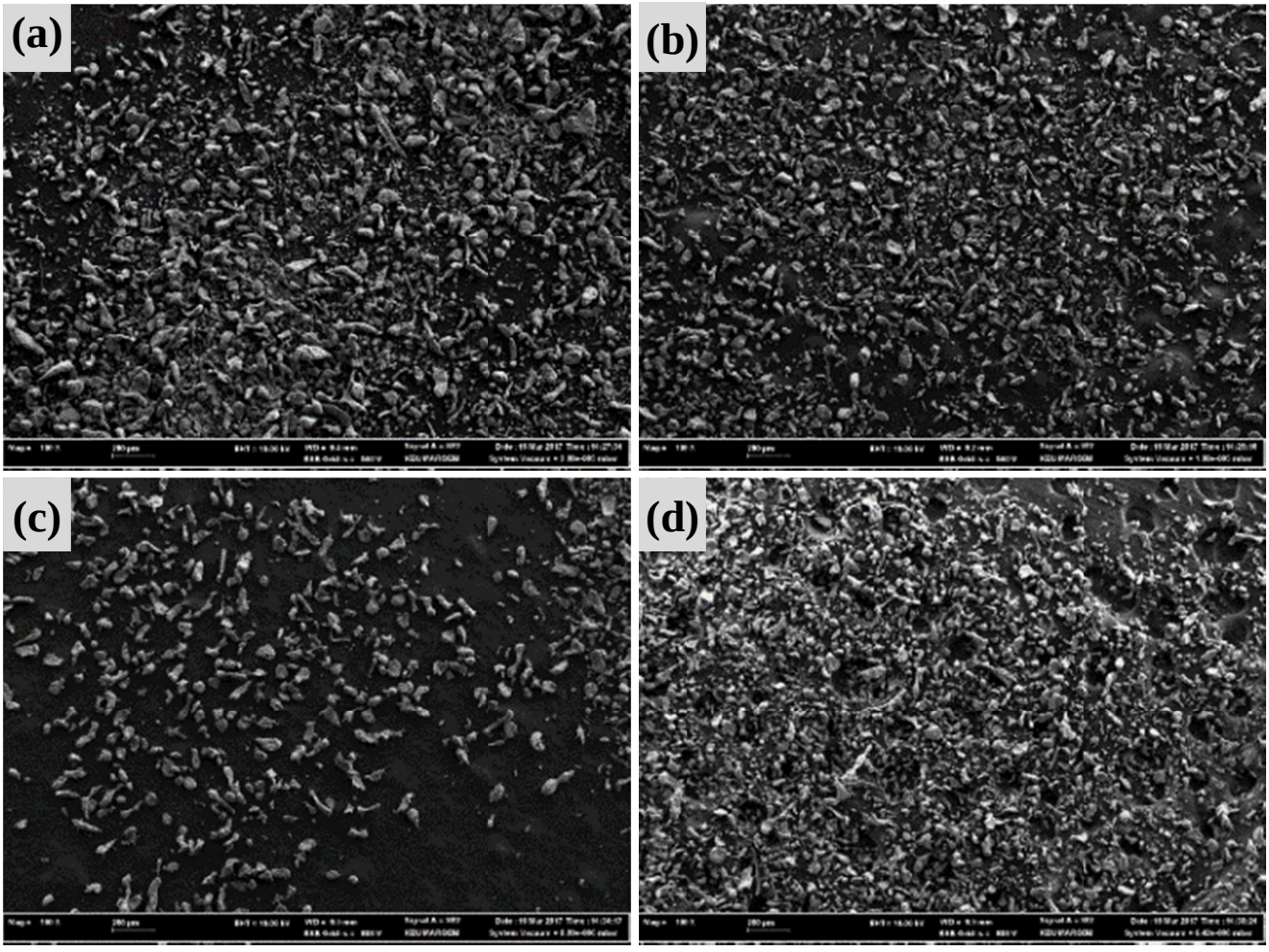

Fig. 2. SEM images of AZ91 alloy powders produced at different gas pressures a) 0.5 MPa b) 1.5 MPa c) 2.5 MPa d) 3.5 MPa

exist under the 3.5 MPa gas pressure. In their study about the effect of Pb during the solidification of AZ91 alloy, Baram et al., emphasized that there was never a back pressure in the nozzle under 3.0 MPa gas pressure [28]. It is seen in this table that the powder size reduced as the gas pressure increased.

TABLE 2

Size values of AZ91 powders

Gas Pressure (MPa)	Dv (10) µm	Dv (50) µm	Dv (90) µm	Span	Specific Surface Area (m^2/kg)
0,5	50,5	155	344	1,897	85,18
1,5	34,6	77,4	161	1,635	99,89
2,5	25,9	72,9	156	2,334	115,9
3,5	24,2	66,6	160	2,046	127,9

Smaller powder production was performed since there is more energy transfer to the melt metal as the gas pressure increased. As is seen in Table 2, powder size decreased as the gas pressure increased. The 50% of powders size at constant temperature of 820°C and different gas pressures was obtained as 66.6 µm at 2 mm nozzle diameter and 3.5 MPa gas pressure. Generally, while 10% of the powders produced for these variables were below 24.2 µm, 90% were composed of powders less than 160 µm. It was determined that at least 10% of the produced powders were composed of powders below 10 µm, but it was not possible to measure these powders since they were coated both on the atomization tower and cyclones and on the containers storing the powders.

3.2. Shape and surface form of the powders

Fig. 2 shows SEM images of AZ91 powders produced at different gas pressures by gas atomization.

When the general appearance of the produced AZ91 alloy powders was examined, it was observed that the powders had ligament, acicular, droplet, flake and spherical shapes, but the shapes of the powders mostly turned to flake, droplet and spherical depending on gas pressure. The powders produced especially in a 3.5 MPa gas pressure and whose SEM image is given in Fig. 2d significantly decreased and it was evident that their shapes were of dropleted and spherical. In the study conducted by Fischmeister et al., [29] on the solidification of gas atomized high-speed steels it was found that the most important parameter forcing a liquid droplet to become spherical was the surface tension. When Fig. 3 was examined, a small proportion of the powder was seen to be spherical. The most important reason for this was associated with the fact that the atomization tower was not at the sufficient height. This is because the powder particles solidified by hitting onto the base of the atomization tower before they could find time to become spherical.

When the powders randomly solidified under the effect of atomization were examined in detail, it was observed that small particle powders formed a satellite on large particle powders. Satellization process occurs as a result of collision of the small

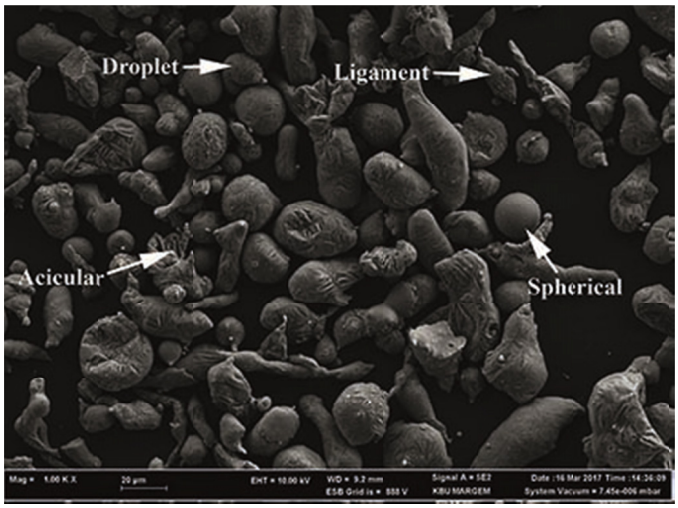

Fig. 3. SEM image showing the general appearance of AZ91 powder produced in 2.5 MPa gas pressure

powder particles with the large powder particles, which have not yet completed the solidification process, during atomization [22,29]. The difference between the solidification times of powders forming at large and small sizes and the acceleration of droplets at different sizes in different ratios by the effect of atomization gas lead to the satellization process [18,30]. Satellization was also observed in the coatings formed by collision of powder and liquid droplets. Such satellization occurred as is seen in the SEM images given in Fig. 4 and Fig. 5; on the other hand, it was observed that the satellization formed by partial coating the powder by droplet or by the complete coating of the droplet by powder [31]. The spiral satellization seen in Fig. 5 is a good example for this.

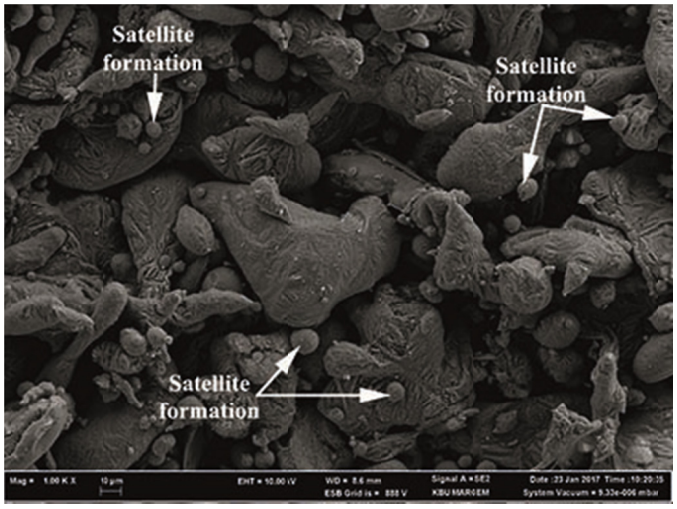

Fig. 4. SEM image of AZ91 powder produced in 3.5 MPa gas pressure

On the other hand, when the satellization in Fig. 5 was examined, it was observed that the satellites were generally formed by the powders below 10 µm and most of these powders were composed of spherical particles. The early solidification of small powders and the collisions of large powders while still in liquid

form cause the formation of satellization. Spherical satellites was thought to be associated with very large contact surface areas and having time to become spherical to reduce the surface energy.

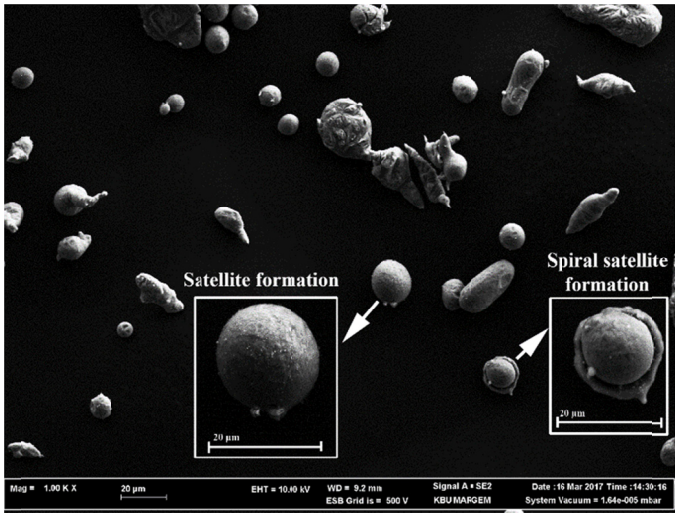

Fig. 5. SEM image of AZ91 powder produced in 3.5 MPa gas pressure

In addition, Fig. 6 shows SEM images taken from surfaces of the atomized powders at 15000X magnification. When the powders produced were examined, it was observed that surface images of the powders also changed depending on the change of gas pressure and the powder surfaces had dendritic or cellular-dendritic microstructure.

It is clearly seen in Fig. 6 that the powder surfaces were porous and the amount of pores decreased depending on the gas pressure. In addition, when the surfaces were carefully examined, it can be noticed that a powder particle (such as in solidification) was formed by the sub particles and the sub particles got smaller with increasing gas pressure. The reason for this can be interpreted as the increase of the nucleation forming the sub-particles depending on the solidification rate as in the solidification of the liquid metal and as the fact that the structure was formed by smaller particles. On the other hand, it was understood from SEM images that the increased gas pressure increased the pressure on the unit surface and a denser surface formed due to the faster cooling of the surface.

3.3. X-Ray diffraction (XRD) and X-Ray fluorescence (XRF) analyses of the powders

Fig. 7 shows the XRD graph of the atomized AZ91 alloy powder and Table 3 shows its XRF chemical analysis results.

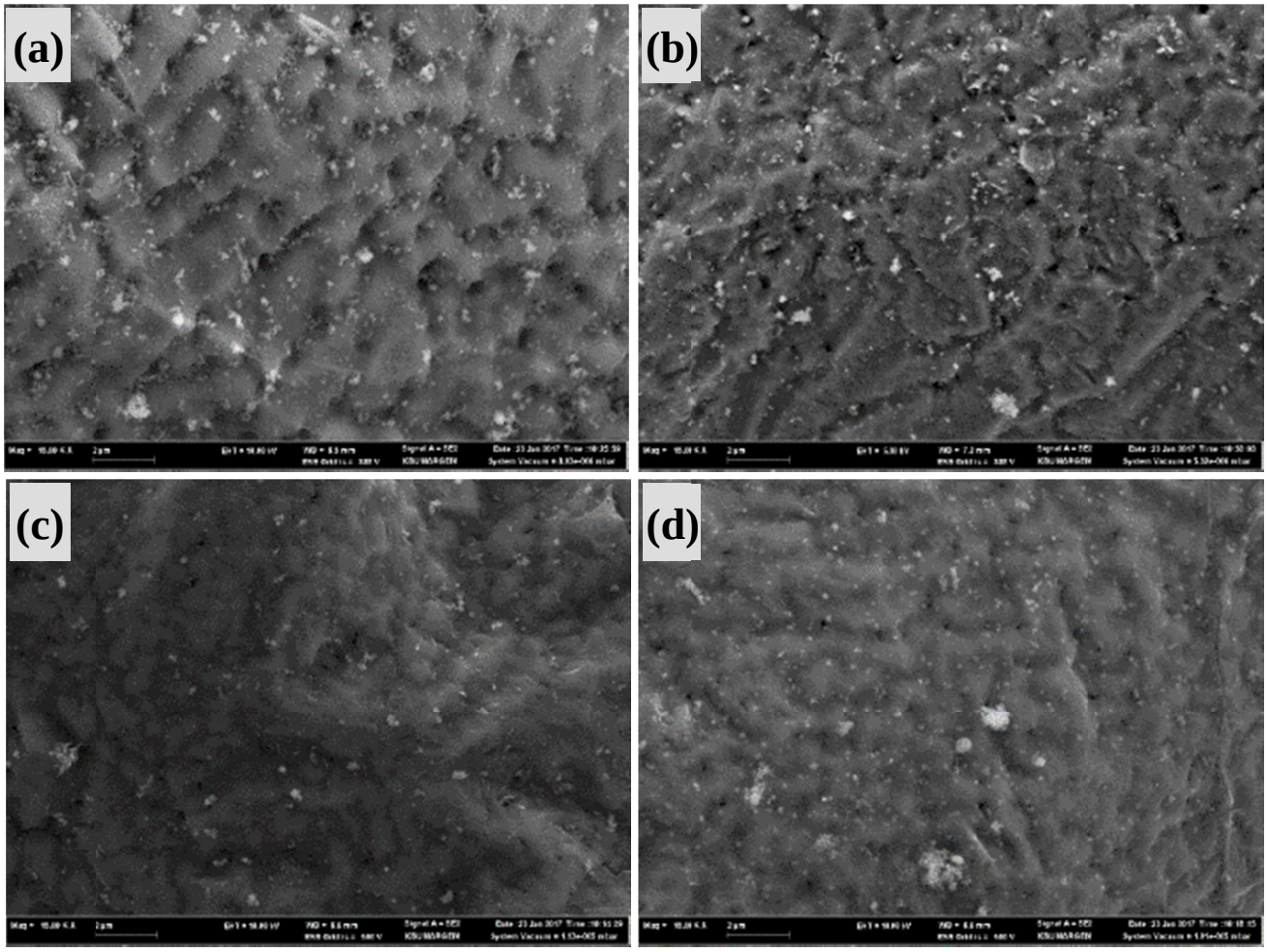

Fig. 6. SEM images of AZ91 alloy powders produced at different gas pressures a) 0.5 MPa b) 1.5 MPa c) 2.5 MPa d) 3.5 MPa

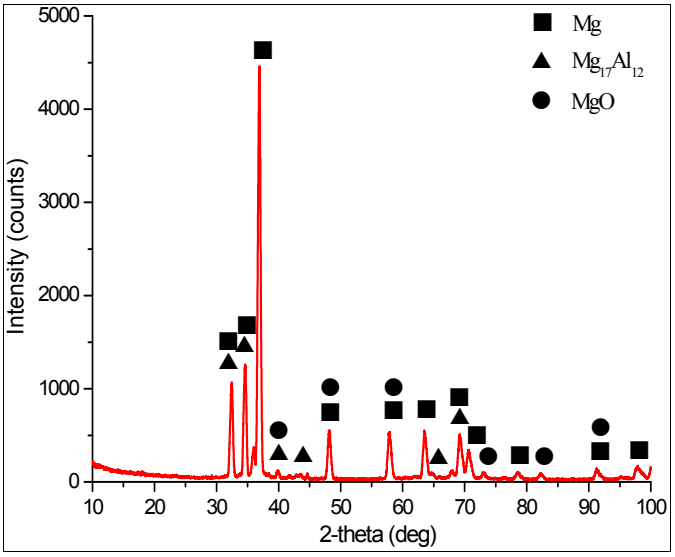

Fig. 7. XRD graph of the produced AZ91 alloy powder

TABLE 3

Chemical (XRF) analysis results of the produced AZ91 alloy powders

Element	Content (%)
Mg	89,6732
Al	8,2790
Zn	1,2084
Mn	0,4024
Fe	0,0330
Ni	0,0087

In XRD pattern of AZ91 alloy, Mg which is the α (main phase) phase and β (intermediate phase) phase along with a very small amount (0.30%) of magnesium oxide (MgO) phase were determined (Fig. 7). It was thought that the magnesium oxide phase formed during open-air contact after solidification. This is because constant argon gas was supplied to the system during melting and atomization.

AZ91 alloy, whose chemical analysis is presented in Table 3, contained 89.67 wt % Mg, 8.27 wt % Al and 1.20 wt % Zn. In addition, trace amounts of Mn, Fe, and Ni were also observed. It is seen in XRD results given in Fig. 7 that Mg and Al combined to form $Mg_{17}Al_{12}$ precipitate. Grant and Daloz [32,33] stated in their study on solidification of Al and Mg that $Mg_{17}Al_{12}$ compound formed depending on the solidification path. As is seen in Fig. 8, AZ91 included hexagonal close packing α-Mg and eutectic $\alpha+\gamma$ (γ phase is named as volume-centered cubic β-$Mg_{17}Al_{12}$ phase) phases [34,35].

Through SEM and EDX studies performed to determine the phases forming during the atomization, α-Mg and β ($Mg_{17}Al_{12}$) phases in the internal structure are seen in Fig. 8. As a result of EDX analysis taken from the points coded with numbers 2 and 5 in Fig. 8, α phase was shown to contain 90.29% Mg, 7.82% Al and 1.88% Zn during the solidification. The result of EDX analysis taken from the point coded with numbers 1 and 4 in Fig. 8 showed that it consisted of β ($Mg_{17}Al_{12}$) phase, an intermetallic compound with 50.2% Mg, 48.04% Al, 1.16% Zn, and 0.57% Mn. The result of EDX analysis taken from the zone shown with number 3 in Fig. 8 gave AZ91 alloy forming the main structure.

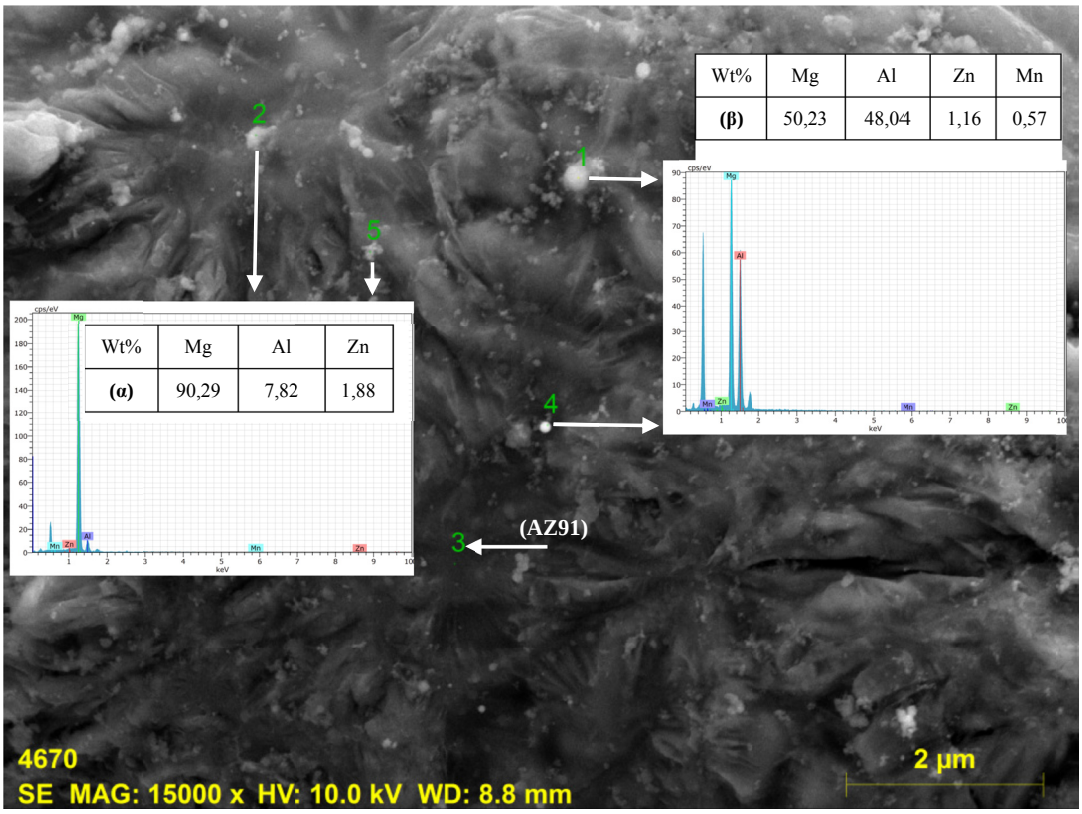

Fig. 8. EDX analysis of α and β phases determined on the SEM image

3.4. Microhardness measurement values of the powders

Six different hardness measurements were made from the samples which were pelletized in the cold pressing device and the averages of these hardness values were taken. As a result of measurements made by the Vickers method under a load of 0.5 g, the hardness. When the results were examined, AZ91 alloy powders produced at different parameters had average hardness values of 110-115 $HV_{0.5}$. These results showed that it had no effect on the hardness of the powders produced depending on the gas pressure.

4. Conclusions

The following results were obtained in this study conducted on the characterization of AZ91 powder produced by the gas atomization method applying different parameters.

1. Powders in different shapes and sizes were obtained with gas atomization method. The smallest powder size was obtained at 820°C, in 2 mm nozzle diameter and at 3.5 MPa pressure.
2. It was observed that the powder size decreased for $D_{v,50}$ from 155 μm to 66,6 μm depending on the increasing gas pressure (Table 2).
3. With increasing gas pressure, it was found that the powder shape changed from the ligament and the acicular to the droplet and spherical structure. Shares of individual kinds of shape of obtained powder were determined in relation to total surface of the material.
4. It was observed that during the atomization different shapes of satellization occurred with the collision of powder and droplets in the 3.5 MPa atomization gas pressure.
5. It was found that the surfaces of the produced powders changed depending on the gas pressure and had a dendritic or cellular dendritic structure.
6. It was determined from XRD and XRF results that the produced AZ91 alloy powder was composed of α and β ($Mg_{17}Al_{12}$) phases and there was a little amount of MgO phase in the structure.
7. Gas pressure was determined not to have any serious effect on the hardness of the produced AZ91 alloy powder.

Acknowledgement

This work was supported by Scientific Research Projects Coordination Unit of Karabük University. Project Number: KBÜ-BAP-15/2-DR-001.

REFERENCES

[1] M.K. Kulekci, The International Journal of Advanced Manufacturing Technology **39** (9), 851-865 (2008).

[2] K. Cho, T. Sano, K. Doherty, C. Yen, G. Gazonas, J. Montgomery, R. DeLorme, Army Research Lab Aberdeen Proving Ground Md (2009).

[3] K.K. Deng, J.C. Li, K.B. Nie, X.J. Wang, J.F. Fan, Materials Science and Engineering A **624**, 62-70 (2015).

[4] M. Forsyth, P.C. Howlett, S.K. Tan, D.R. MacFarlane, N. Birbilis, Electrochemical and solid-state letters **9** (11), B52-B55 (2006).

[5] F. Czerwinski, Corrosion Science **86**, 1-16 (2014).

[6] W. Zhang, B. Tian, K.Q. Du, H.X. Zhang, F.H. Wang, Int. J. of Electrochemical Science **6**, 5228-5248 (2011).

[7] M. Yıldırım, D. Özyürek, Materials & Design **51**, 767-774 (2013).

[8] G. Neite, K. Kubota, K. Higashi, F. Hehmann, Materials science and technology (1996).

[9] D.H. StJohn, M.A. Qian, M.A. Easton, P. Cao, Z. Hildebrand, Metallurgical and Materials Transactions A **36** (7), 1669-1679 (2005).

[10] M. Qian, A. Das, Scripta materialia **54** (5), 881-886 (2006).

[11] D. Vinotha, K. Raghukandan, U.T.S. Pillai, B.C. Pai, Transactions of the Indian Institute of Metals **62**(6), 521-532 (2009).

[12] M. Mondet, E. Barraud, S. Lemonnier, J. Guyon, N. Allain, T. Grosdidier, Acta Materialia **119**, 55-67 (2016).

[13] B. Han, D. Gu, Y. Yang, L. Fang, G. Peng, C. Yang, International Journal Of Electrochemical Science **12** (1), 374-385 (2017).

[14] L. Čížek, M. Greger, L. Pawlica, L.A. Dobrzański, T. Tański, Journal of Materials Processing Technology **157**, 466-471 (2004).

[15] C.L. Mendis, K. Hono, 4-Understanding precipitation processes in magnesium alloys, M.O. Pekguleryuz, K.U. Kainer, A.A. Kaya (Eds.), Fundamentals of Magnesium Alloy Metallurgy 125-151 (2013).

[16] M.M. Avedesian, H. Baker, ASM Speciality Handbook: Magnesium and Magnesium alloys. ASM International **59**, 60 (1999).

[17] R.M. German, Powder Metallurgy Science MPIF-Metal Powder Industries Federation. Princeton, USA (1994).

[18] A. Lawley, Atomization: the production of metal powders. Metal Powder Industries Federation, 1105 College Rd. East, Princeton, New Jersey 08540-6692, USA, 159 (1992).

[19] S. Buytoz, F. Dagdelen, S. Islak, M. Kok, D. Kir, E. Ercan, Journal of Thermal Analysis and Calorimetry **117** (3), 1277-1283 (2014).

[20] S. Islak, S. Buytoz, O. Eski, Journal Of Optoelectronics And Advanced Materials **17** (1-2), 211-215 (2015).

[21] S. Islak, E. Çelik, D. Kir, C. Özorak, Russian Journal of Non-Ferrous Metals **57** (4), 374-380 (2016).

[22] E. Klar, J.W. Fesko, Gas and water atomization. Metals handbook **7**, 25-39 (1984).

[23] Ş. Karagöz, R. Yamanoğlu, Ş.H. Atapek, Journal of Engineering and Architecture Faculty of Eskişehir Osmangazi University **22** (3) (2009).

[24] Ş. Oğuz, Z. Öztürk, E. Uzun, A. Kurt, M. Boz, 6th International Advanced Technologies Symposium (IATS'11), 565, (2011).

[25] M. Aydın, R. Ünal, Makine Teknolojileri Elektronik Dergisi **1**, 69-76 (2007).

[26] H. Gökmeşe, B. Bostan, Gazi Üniversitesi Fen Bilimleri Dergisi Part C: Tasarım ve Teknoloji **1** (1), 1-8 (2013).

[27] I. Uslan, S. Kucukarslan, Journal Of The Faculty Of Engineering And Architecture Of Gazı University **25** (1), 1-8 (2010).

[28] J. Baram, Materials Science and Engineering **98**, 65-69 (1988).
[29] H.F. Fischmeister, A.D. Ozerskii, L. Olsson, Powder metallurgy **25** (1), 1-9 (1982).
[30] T.W. Clyne, R.A. Ricks, P.J. Goodhew, International Journal of Rapid Solidification **1** (1), 59-80 (1984).
[31] A.J. Aller, A. Losada, Powder Metall. Int. **21** (5), 15-19 (1989).
[32] N.J. Grant, Metallurgical and Materials Transactions A **23** (4), 1083-1093 (1992).
[33] D. Daloz, G. Michot, International Journal of Rapid Solidification **9** (4), 289-304 (1996).
[34] J.M. Zhang, B.L. Jıang, Z.H. Wang, S. Yuan, H.Q. Nan, H.B. Luo, Research & Development, (2007).
[35] A. Boby, U.T.S. Pillai, B.C. Pai, Transactions of the Indian Institute of Metals **66** (2), 105-108 (2013).